

Effect of Annealing Temperature on the Properties of ITO/Au/ITO Films

Joo Hyun Chae and Daeil Kim[†]

Department of Materials Science and Engineering, University of Ulsan,
San 29, Mugeo-Dong, Nam-Gu, Ulsan, Korea, 680-249

(Received November 12, 2008 : Received in revised form December 17, 2008 : Accepted December 23, 2008)

Abstract Transparent Sn-doped In₂O₃ (ITO) single-layer and ITO/Au/ITO multilayer films were deposited on glass substrates by reactive magnetron sputtering to compare the properties of the films. They were then annealed in a vacuum of 1×10^{-2} Pa at temperatures ranging from 150 to 450 °C for 20 min to determine the effect of the annealing temperature on the properties of the films. As-deposited 100 nm thick ITO films exhibit a sheet resistance of 130 Ω/□ and optical transmittance of 77% at a wavelength length of 550 nm. By inserting a 5 nm-thick Au layer in ITO/metal/ITO (IMI) films, the sheet resistance was decreased to as low as 20 Ω/□ and the optical transmittance was decreased to as little as 73% at 550 nm. Post-deposition annealing of ITO/Au/ITO films led to considerably lower electrical resistivity and higher optical transparency. In the X-ray diffraction pattern, as-deposited ITO films did not show any diffraction peak, whereas as-deposited ITO/Au/ITO films have Au (222) and In₂O₃ (110) crystal planes. When the annealing temperature reached the 150 - 450 °C range, the both diffraction peak intensities increased significantly. A sheet resistance of 8 Ω/□ and an optical transmittance of 82% were obtained from the ITO/Au/ITO films annealed at 450 °C.

Key words indium tin oxide, gold, sputtering, annealing.

1. Introduction

Sn-doped In₂O₃ (ITO) film is a degenerated wide-gap semiconductor with good electrical conductivity and high optical transmission across the visible spectrum.¹⁾ Due to their unique properties, ITO films have many applications, such as solar cells and gas sensors.^{2,3)} In order to deposit high-quality ITO films, various research works using magnetron sputtering have been performed to optimize substrate temperature, sputtering power, and reactive gas flow rate.⁴⁻⁶⁾

In recent years, M. Bender and A. Kloppel *et al.* reported several advantages of magnetron-sputtered ITO/metal/ITO (IMI) structures that use interlayer Ag⁷⁾ and AgCu⁸⁾ to improve the structural and optoelectrical properties of ITO films.

In this study, a sandwich structure of ITO/Au/ITO films was deposited on glass substrates by radio-frequency (RF) sputtering of ITO and direct current (DC) sputtering of Au intermediate film. ITO single-layer films, which have the same thickness of 100 nm, were deposited under the same conditions as for

the ITO/Au/ITO films to compare the structural and optoelectrical properties. After comparison of the properties of as-deposited films, the ITO/Au/ITO films were post-deposition annealed at different temperatures in a vacuum and then the effects of annealing temperature on the structural and optoelectrical properties of the films were investigated.

2. Experimental procedure

Deposition of ITO and ITO/Au/ITO films was performed on glass substrate (size; 7×7 cm²) in a reactive magnetron sputtering system equipped with two cathodes. Fig. 1 shows the schematic diagram of sputtering system. The RF (13.56 MHz) and DC power were applied to ITO (Purity; 99.99%) and Au (Purity; 99.9%) targets, respectively. The target had a 3-in diameter by 0.25-in thick sintered In₂O₃ (90 wt%) + SnO₂ (10 wt%) and pure Au disk. The substrates were ultrasonically cleaned in acetone and methanol, rinsed in de-ionized water, and then dried in flowing nitrogen gas before deposition. Prior to deposition, the chamber was evacuated to 1.3×10^{-4} Pa.

ITO films were deposited at 3×10^{-1} Pa in an argon (Ar) and oxygen (O₂) gas mixture, and the

[†]Corresponding author

E-Mail : dkim84@ulsan.ac.kr(D. Kim)

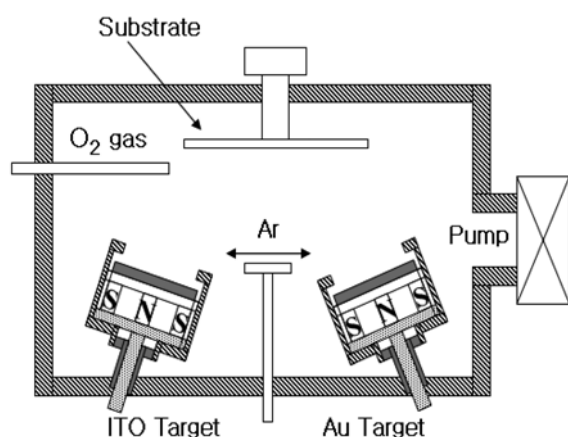


Fig. 1. Schematic diagram of a magnetron sputtering system.

Au intermediated films were deposited in a pure Ar atmosphere of 1×10^{-1} Pa. A deposition distance of 10 cm between the target and substrate was maintained throughout deposition, and the substrate rotation speed was set to 10 rpm. The substrate temperature was monitored using a k-type thermocouple in contact with the substrate surface. Although the substrate was not heated intentionally, the substrate temperature was estimated to be near 70 °C due to the plasma heating.

By controlling the deposition time, a thickness of 100 nm was achieved in both ITO and in ITO 50 nm/Au 5 nm/ITO 45 nm multilayer films. After deposition, ITO/Au/ITO films were annealed in a vacuum of 1×10^{-2} Pa for 20 min at 150, 300, and 450 °C. The film thickness was confirmed with a surface profilometer. Over a wavelength interval from 300 to 800 nm, optical absorption and transmittance were measured by a UV-Vis Spectrophotometer (Carry100 Cone, Varian). The data presented in this work referred to the transmission of the multilayer, including the glass substrate. The optical transmittance of the bare glass substrate was also measured for comparison. In this study, all transmittance values included the glass substrate, which had an optical transmission of nearly 90%. High resolution XRD (X'pert PRO, Philips) at the Korea Basic Science Institute (KBSI) was used to observe thin film crystallinity.

The electrical properties were measured by four point probe (MCP-T360, Mitsubishi) at room temperature. The performance of as-deposited films and post-deposition vacuum-annealed films were evaluated using a figure of merit (ϕ_{TC}).⁹ The ϕ_{TC} is defined as $\phi_{TC} = T^{10}/R_s$ where

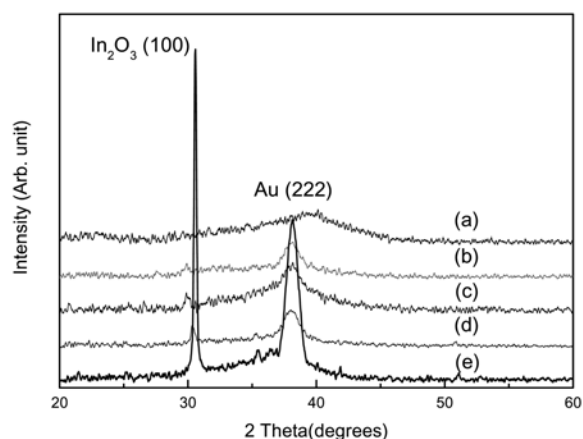


Fig. 2. The XRD pattern of as deposited and post deposition annealed films. (a) ITO single-layer film, (b) ITO/Au/ITO films, (c) Annealed ITO/Au/ITO films at 150 °C, (d) Annealed ITO/Au/ITO films at 300 °C, (e) Annealed ITO/Au/ITO films at 450 °C.

T is the optical transmittance at 550 nm in this study and R_s is the sheet resistance.

3. Results and discussion

It is well known that the ITO films deposited by magnetron sputtering at low temperature are usually amorphous.¹⁰ Recently Sun *et al.* investigated the initial growth mode of ITO on a glass substrate over a substrate temperature range of 20–400 °C and then they reported that an amorphous structure ITO film was formed at substrate temperatures below 150 °C. Similarly Jung *et al.* found that ITO/Ag/ITO films also required a high substrate temperature or post-deposition annealing temperature of 300 °C to provide the polycrystalline structures that ensured high optoelectrical properties.^{11,12}

Fig. 2 shows the XRD pattern of as-deposited and post-deposition annealed films. As-deposited ITO films (a) did not exhibit any diffraction peaks, whereas ITO/Au/ITO films (b) which deposited without intentional substrate heating showed diffraction peaks corresponding to Au (222) and In_2O_3 (100) planes. This means that the Au intermediated layer is very effective in crystallizing ITO films. When the annealing temperature reached 150–450 °C, the intensities of the In_2O_3 (100) peak in films (c), (d), and (e) increased, and the full width at half maximum (FWHM) decreased. The FWHM for In_2O_3 (100) peak decreased to 0.3° for (c), 0.2° for (d), and 0.1° for (e) due to crystallization.

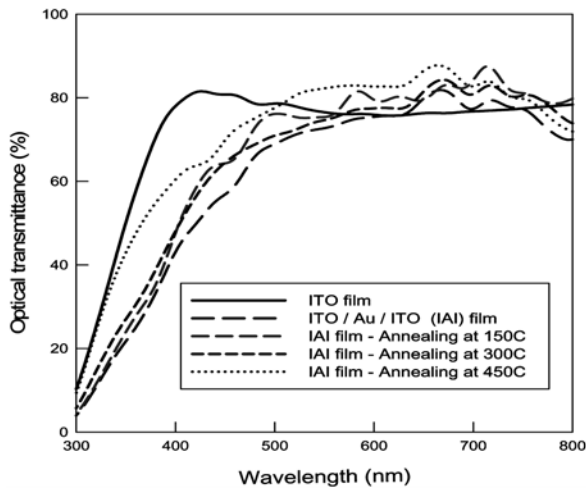


Fig. 3. Optical transmittance of as deposited and post deposition annealed films.

Table 1. Comparison of sheet resistance (R_s , Ω/\square) and figure of merit (ϕ_{TC} , $10^{-3}\Omega^{-1}$) of ITO and ITO/Au/ITO (IAI) films.

Films	R_s	ϕ_{TC}
ITO single-layer films	130	1.5
ITO/Au/ITO films	21	5.2
Annealed IAI films at 150 °C	15	10.0
Annealed IAI films at 300 °C	11	14.4
Annealed IAI films at 450 °C	8	49.2

From the XRD patterns, it can be supposed that In_2O_3 (100) grain size is increased with annealing temperature. Since larger grain size results in a lower density of the grain boundary, the grain size is related to the resistivity because the grain boundary acts as a barrier for carrier conduction. Therefore, it can be speculated that the resistivity decreased with increased annealing temperature due to increased grain size.

The influence of the Au interlayer in an IMI structure and the annealing temperature on the sheet resistance (R_s) of the films is investigated, respectively. The ITO films exhibit the R_s of $130 \Omega/\square$, higher than that of ITO/Au/ITO films. Inserting 5-nm thick Au film between ITO films, the R_s decreases to $21 \Omega/\square$. As annealing temperature increases up to 450 °C, the R_s decrease to as little as $8 \Omega/\square$.

Fig. 3 shows the optical transmittance of as-deposited films and post-deposition annealed ITO/Au/ITO films. ITO films exhibit 77% optical transmission at 550 nm, while ITO/Au/ITO films annealed at 450 °C had the highest optical transmittance, 82%, at 550 nm. The ϕ_{TC} for as-deposited films and annealed films are

compared in Table 1. The ϕ_{TC} reaches a maximum of $1.7 \times 10^{-2} \Omega^{-1}$ for ITO/Au/ITO films annealed at 450 °C. Since higher ϕ_{TC} means better quality of TCO films,¹³⁾ it can be concluded that ITO/Au/ITO films have better optoelectrical properties than ITO films do, and the post-deposition annealing process for ITO/Au/ITO films is very effective for improving the optoelectrical properties of the films.

4. Conclusion

ITO single-layer films and a sandwich structure of ITO 50 nm /Au 5 nm /ITO 45 nm films were deposited by magnetron sputtering to investigate the effect of the Au interlayer on the properties of the films. Also, ITO/Au/ITO films were post-deposition vacuum annealed to consider the annealing effects on the properties of the ITO/Au/ITO films. A sandwich structure of ITO/Au/ITO films shows a lower sheet resistance of 21Ω , than that of the as-deposited ITO films (130Ω). When the annealing temperature reached 150–450 °C range, XRD peak intensities of In_2O_3 (100) and Au (222) were increased significantly. The ITO/Au/ITO films annealed at 450 °C exhibit two orders of magnitude higher figure of merit (Φ_{TC}) ($1.7 \times 10^{-2} \Omega^{-1}$) than those of as-deposited ITO films ($7.3 \times 10^{-4} \Omega^{-1}$).

References

1. D. Kim and S. Kim, *Thin Solid Films*, **408**, 218 (2002).
2. B. Yoo, K. Kim, S. Lee, W. Kim and N. Park, *Sol. Ener. Mater. and Sol. Cells*, **92**, 873 (2008).
3. V. Vaishnav and P. Patel, *Thin Solid Film*, **490**, 94 (2005).
4. H. Omoto, A. Takamatsu and T. Kobayashi, *Vacuum*, **80**, 783 (2006).
5. T. Minami, S. Ida, T. Miyata, *Thin Solid Film*, **416**, 92 (2002).
6. M. Bender, W. Seelig, C. Daube, H. Frankenberger, B. Ocker and J. Stollenwerk, *Thin Solid Films*, **326**, 72 (1998).
7. M. Bender, W. Seelig, C. Daube, H. Frankenberger, B. Ocker and J. Stollenwerk, *Thin Solid Films*, **326**, 67 (1998).
8. A. Kloppel, W. Riegseis, B. Meyer, A. Charmann, C. Aube, J. Stollenwerk and J. Rube, *Thin Solid Films*, **365**, 139 (2000).
9. G. Haacke, *J. Appl. Phys.*, **47**, 4086 (1976).
10. K. Zhang, F. Zhu, C. H. A. Huan and A. Wee, *Thin Solid Film*, **376**, 255 (2000).
11. X. Sun, H. Huang and H. Kwon, *Appl. Phys. Lett.*, **68**, 2663 (1996).
12. Y. Jung, Y. Choi, H. Lee and D. Lee, *Thin Solid Film*, **440**, 278 (2003).
13. H. J. Park, J. H. Chae and D. Kim, *Vacuum*, **83**, 448, (2008).